Original Article | Technology, Experiment, and Physics

eISSN 2005-8330
https://doi.org/10.3348/kjr.2020.1455
Korean J Radiol 2021;22(10):1708-1718

Korean Journal of Radiology
KJR

Investigation of the Characteristics of New, Uniform, Extremely Small Iron-Based Nanoparticles as T1 Contrast Agents for MRI

Young Ho So[1, 2], Whal Lee[2, 3, 4], Eun-Ah Park[2, 3], Pan Ki Kim[5]

[1]Department of Radiology, SMG-SNU Boramae Medical Center, Seoul, Korea; [2]Department of Radiology, Seoul National University College of Medicine, Seoul, Korea; [3]Department of Radiology, Seoul National University Hospital, Seoul, Korea; [4]Institute of Radiation Medicine, Seoul National University Medical Research Center, Seoul, Korea; [5]Department of Radiology and Research Institute of Radiological Science, Severance Hospital, Yonsei University College of Medicine, Seoul, Korea

Objective: The purpose of this study was to evaluate the magnetic resonance (MR) characteristics and applicability of new, uniform, extremely small iron-based nanoparticles (ESIONs) with 3–4-nm iron cores using contrast-enhanced magnetic resonance angiography (MRA).

Materials and Methods: Seven types of ESIONs were used in phantom and animal experiments with 1.5T, 3T, and 4.7T scanners. The MR characteristics of the ESIONs were evaluated via phantom experiments. With the ESIONs selected by the phantom experiments, animal experiments were performed on eight rabbits. In the animal experiments, the *in vivo* kinetics and enhancement effect of the ESIONs were evaluated using half-diluted and non-diluted ESIONs. The between-group differences were assessed using a linear mixed model. A commercially available gadolinium-based contrast agent (GBCA) was used as a control.

Results: All ESIONs showed a good T1 shortening effect and were applicable for MRA at 1.5T and 3T. The relaxivity ratio of the ESIONs increased with increasing magnetic field strength. In the animal experiments, the ESIONs showed peak signal intensity on the first-pass images and persistent vascular enhancement until 90 minutes. On the 1-week follow-up images, the ESIONs were nearly washed out from the vascular structures and organs. The peak signal intensity on the first-pass images showed no significant difference between the non-diluted ESIONs with 3-mm iron cores and GBCA ($p = 1.000$). On the 10-minutes post-contrast images, the non-diluted ESIONs showed a significantly higher signal intensity than did the GBCA ($p < 0.001$).

Conclusion: In the phantom experiments, the ESIONs with 3–4-nm iron oxide cores showed a good T1 shortening effect at 1.5T and 3T. In the animal experiments, the ESIONs with 3-nm iron cores showed comparable enhancement on the first-pass images and superior enhancement effect on the delayed images compared to the commercially available GBCA at 3T.

Keywords: *Iron oxide nanoparticle; Blood pool contrast agent; Magnetic resonance angiography; Contrast enhancement*

Received: December 13, 2020 **Revised:** April 6, 2021 **Accepted:** May 10, 2021

This study was supported by a grant from the Hanwha Chemical Corp., the Bio & Medical Technology Development Program of the National Research Foundation (NRF) funded by the Korean government (MSIT) (No. 2017M3A9G5082641), and the Korea Health Technology R&D Project through the Korea Health Industry Development Institute (KHIDI), funded by the Ministry of Health & Welfare, Republic of Korea (grant number: HI20C2092).

Corresponding author: Whal Lee, MD, PhD, Department of Radiology, Seoul National University Hospital, Seoul National University College of Medicine, Institute of Radiation Medicine, Seoul National University Medical Research Center, 101 Daehak-ro, Jongno-gu, Seoul 03080, Korea.

• E-mail: whal.lee@gmail.com

Korean Journal of Radiology
KJR

INTRODUCTION

Since the recent introduction of 3 tesla (T) magnetic resonance (MR) scanners and the application of three-dimensional (3D) gradient echo sequences, contrast-enhanced magnetic resonance angiography (MRA) has become an accurate technique for the evaluation of most vascular structures [1-3]. Contrast-enhanced MRA is usually performed using gadolinium-based blood pool agents, and the spatial resolution of MR images can be improved owing to the T1 shortening effect [4,5]. However, owing to the potential toxicity of gadolinium ions, they must be bound to ligands for use as a contrast agent. The half-life of gadolinium-based contrast agents (GBCAs) is approximately 90 minutes in patients with normal renal function but is prolonged from 30 to 120 hours in patients with chronic renal failure. During this time, dissociated gadolinium ions can compete with calcium ions and cause nephrogenic systemic fibrosis (NSF). Therefore, several reports and cases have indicated that GBCAs were the causative agents of NSF in patients with severe renal impairment or those receiving dialysis; according to these studies, most of the reported NSF occurred in patients who received older linear GBCAs [6-8]. Recently, the incidence of NSF has decreased considerably with the use of macrocyclic GBCAs. However, it has also been attributed to the avoidance of GBCA use in high-risk patients and excessive dose administration [9-11].

Recently, ultrasmall superparamagnetic iron oxides (USPIOs), which have a crystalline iron oxide core of less than 50 nm and dextran coating, were introduced in contrast-enhanced MRA. USPIOs exhibit a T1 shortening effect owing to the reduction in the volume magnetic anisotropy and spin disorders on the surface of the nanoparticles [12]. In addition, the dextran coating of USPIOs prevents endocytosis by macrophages, permitting a long plasma half-life [13,14]. With these properties, the possibility of using USPIOs as an alternative blood pool MR contrast agent has emerged. However, the previously reported nanoparticles were larger than 4 nm and still showed considerable magnetic moment, resulting in perturbation of the magnetic field and blooming effect.

With the recent advances in synthetic methods, the size reduction of magnetic nanoparticles to 3–4 nm has become possible with more stability in the magneto-crystalline phase and the surface state, resulting in the maximized T1 shortening effect of the magnetic nanoparticles.

The purpose of this study was to evaluate the MR characteristics and applicability of new, uniform, extremely small iron-based nanoparticles (ESIONs) with 3–4-nm iron cores in contrast-enhanced MRA through phantom and animal experiments.

MATERIALS AND METHODS

This study was approved by our institutional animal care and use committee (IRB No. SNUH IACUC 11-0145).

Characteristics of the ESIONs

Seven different types of ESIONs (KEG1–7, Hanwha Chemical Corp.) with 3–4-nm iron oxide nanoparticle cores were used in this study. Structurally, the ESIONs were capped with polyethylene glycol-derivatized phosphine oxide (PO-PEG), which is called the surface ligand. The ligand is composed of a phosphine-oxide head group that strongly binds to the iron oxide nanoparticle core and the hydrophilic polyethylene glycol tail group that will be exposed to the aqueous medium. With the surface ligand, ESIONs could have high colloidal stability and biocompatibility in aqueous media. The ESIONs were synthesized via thermal decomposition of the iron-oleate complex in the presence of oleic acid and oleyl alcohol in diphenyl ether [14]. After synthesis of the ESIONs, ligand exchange with PO-PEG was performed to prevent aggregation and afford hydrophilic properties. After ligand exchange, the ESIONs were dispersed in distilled water. With the surface ligand, the ESIONs finally had a 5–14-nm overall hydrodynamic diameter. The core size, overall size, and maximum concentration of the ESIONs are listed in Table 1.

Table 1. The Iron Core Size, Overall Size, and Maximum Concentration of ESIONs

	Core Size (nm)	Overall Size (mean) (nm)	Maximum Concentration (mmoL/L)
KEG1	3	5	19.73
KEG2	4	6	56.32
KEG3	3	10	66.37
KEG4	4	12	82.87
KEG5	3	13	40.36
KEG6	3	5	18.30
KEG7	3	14	12.74
Gd-DOTA	NA	NA	133.55

ESIONs = extremely small-sized iron oxide nanoparticles, Gd-DOTA = gadoterate meglumine (Dotarem), NA = not avaliable

https://doi.org/10.3348/kjr.2020.1455

MR Relaxivity of the ESIONs

The phantom was prepared with the ESIONs and serial dilutions (1/2, 1/4, 1/8, 1/16, 1/32, 1/64, and 1/128 in normal saline) in 1.5-mL cylindrical tubes. These sample series were lined up in descending order of concentration in a plastic plate with multiple wells. To compare the MR relaxation properties of commercially available contrast media, we used Dotarem® (Gd-DOTA, Guerbet, Roissy CdG) as a control and prepared the sample series in the same manner. To investigate the relaxivity in various magnetic fields, we performed MR imaging using 1.5T (Signa, GE Healthcare), 3T (Tim Trio, Siemens), and 4.7T (BioSpec 47/40, Bruker) MR scanners. The MR room temperature was approximately 22°C.

T1-weighted images were acquired with an inversion-recovery turbo spin-echo sequence at several inversion times (TI) at 1.5T and 3T and with a multislice multiecho (MS-ME) sequence at 4.7T. T2-weighted images were acquired with a multiple echo spin echo sequence with multiple echo times (TE) at 1.5T and 3T and with an MS-ME sequence at 4.7T.

The relaxation curves of the samples were obtained based on various T1- and T2-weighted images, and the T1 and T2 values of the samples were obtained from the relaxation curves.

MR relaxivity (r_1 and r_2) was defined as the slope of the linear regression generated from a plot of the measured relaxation rate (1/T1 and 1/T2) versus the concentration of the contrast media and obtained by curve-fitting the experimental signal intensity (SI) using basic equation (1) or (2):

$$SI\ (TI) = S_0\ (1 - 2e^{-TI/T1}) \quad (1)$$

$$SI\ (TE) = S_0\ (e - e^{-TE/T2}) \quad (2)$$

where SI (TI) or SI (TE) indicates the SI as a function of TI or TE, respectively, and S_0 corresponds to the steady-state SI.

After obtaining the relaxation times, we calculated r_1 and r_2 via linear fitting using equation (3):

$$\frac{1}{Ti\ (measured)} = \frac{1}{Ti\ (solution)} + r_i \times (concentration\ of\ contrast\ material) \quad (3)$$

where Ti (measured) indicates the longitudinal (T1) or transverse (T2) relaxation times of a solution containing contrast material and Ti (solution) indicates the relaxation time of the solvent without contrast material.

The mean SI of the samples was measured using the measurement tool provided by the PACS system (Maroview 5.4, Infinitt). The mean SI was measured under the assumption that the background signal was constant. The region of interest of each sample was located in the middle of the image slice with the largest diameter.

In vivo Kinetics of the ESIONs

To evaluate the *in vivo* kinetics of the ESIONs, we performed MRA with a selected ESION showing a good T1 shortening effect (KEG5). Dotarem® was used as a control for comparison with the commercially available MR contrast media.

Two 40-week-old New Zealand white rabbits (weight, 3 kg) were prepared for MRA. Complete anesthesia was achieved after intramuscular injection of ketamine hydrochloride (100 mg/kg ketamine). The marginal ear vein was catheterized for the delivery of contrast materials using a 24-gauge peripheral intravenous angiocatheter. The animal was placed in the supine position in a standard head coil, and the abdomen was centered in the magnet (3T, Tim Trio, Siemens). The doses of KEG5 and Dotarem® were 0.093 and 0.1 mmoL/kg, respectively. After the pre-contrast images were obtained, the contrast material was infused as a bolus at a constant rate for 10 seconds manually. MRA was performed with the bolus triggering technique at the left ventricle using a 3D fast low-angle shot (FLASH) sequence.

Vascular enhancement, organ enhancement, and clearance of the ESIONs over time were evaluated. MR images were obtained pre- and immediately post-contrast injection; at 3, 5, 10, 20, 40, 60, and 90 minutes post-contrast; and 1 week later. The mean SI of the immediate post-contrast image was measured in the left ventricle, aortic arch, carotid artery, descending thoracic aorta, ascending aorta, right iliac artery, left iliac artery, right kidney cortex and medulla, liver, psoas muscle, and bladder. The mean SI at 3, 5, 10, 20, 40, 60, and 90 minutes post-contrast was measured in the left ventricle and descending thoracic aorta. The mean SI of the target regions was measured using the measurement tool provided by the PACS system (Maroview 5.4, Infinitt). The signal intensities were measured under the assumption that the background signal was constant.

In vivo Cross-Over Experiment

To evaluate the enhancement effect of the ESIONs

https://doi.org/10.3348/kjr.2020.1455

Korean Journal of Radiology
KJR

in contrast-enhanced MRA, we performed a cross-over experiment using two 3-nm ESIONs with different surface ligands (KEG1 and KEG3) and Dotarem® in rabbits. The contrast agents were prepared with a clinical dose and a half-diluted clinical dose: 0.093 mmoL/kg KEG1 and KEG3 (KEG1-S and KEG3-S), 0.047 mmoL/kg KEG1 and KEG3 (KEG1-H and KEG3-H), and 0.1 mmoL/kg Dotarem® (DOT-S) and 0.05 mmoL/kg Dotarem® (DOT-H).

MRA was performed in six 40-week-old New Zealand white rabbits (weight, 3 kg). The animal preparation and MRA protocols were the same as those used in the previous *in vivo* study. MRA was performed with a cross-over design, that is, three contrast materials with two different doses were applied to each rabbit, for a total of six rabbits. The time interval of each MRA in a rabbit was at least 1 week to minimize the effect of the previously admitted contrast material.

MR images were obtained pre- and immediately post-contrast injection and post-contrast at 1, 5, and 10 minutes. The mean SI was measured at the aortic arch and descending thoracic aorta. The mean SI of the target regions was measured using the measurement tool provided by the PACS system (Maroview 5.4, Infinitt). The signal intensities were measured under the assumption that the background signal was constant. Differences in contrast enhancement among the six contrast agents were evaluated.

Statistical analysis for the cross-over experiment was performed to assess between-group differences using a linear mixed model. Differences with adjusted p values of less than 0.05 were considered significant (with Bonferroni's correction). Statistical analysis was performed using R version 3.4.5 (http://r-project.org).

RESULTS

MR Relaxivity of the ESIONs

MR imaging of the phantom was performed, and relaxation curves were obtained based on various T1- and T2-weighted images (Figs. 1, 2). Linear regressions were performed to determine the MR relaxivity (Fig. 3). The calculated relaxivity (r_1 and r_2) and relaxivity ratio (r_2/r_1) at 1.5T, 3T, and 4.7T are listed in Table 2. The highest r_1 relaxivity of the ESIONs was found at 1.5T, and the r_1 relaxivity decreased with increasing magnetic field strength. The r_2 relaxivity of the ESIONs showed no significant change from 1.5T to 3T but increased at 4.7T. The lowest relaxivity ratio (r_2/r_1) of the ESIONs was observed at 1.5T. The relaxivity ratio increased with increasing magnetic field strength. The changes in the r_1 relaxivity and relaxivity ratio (r_2/r_1) showed similar patterns to those of Dotarem®. At 1.5T and 3T, all ESIONs showed relaxivity ratios (r_2/r_1) of 6 or less, indicating good T1 shortening effects.

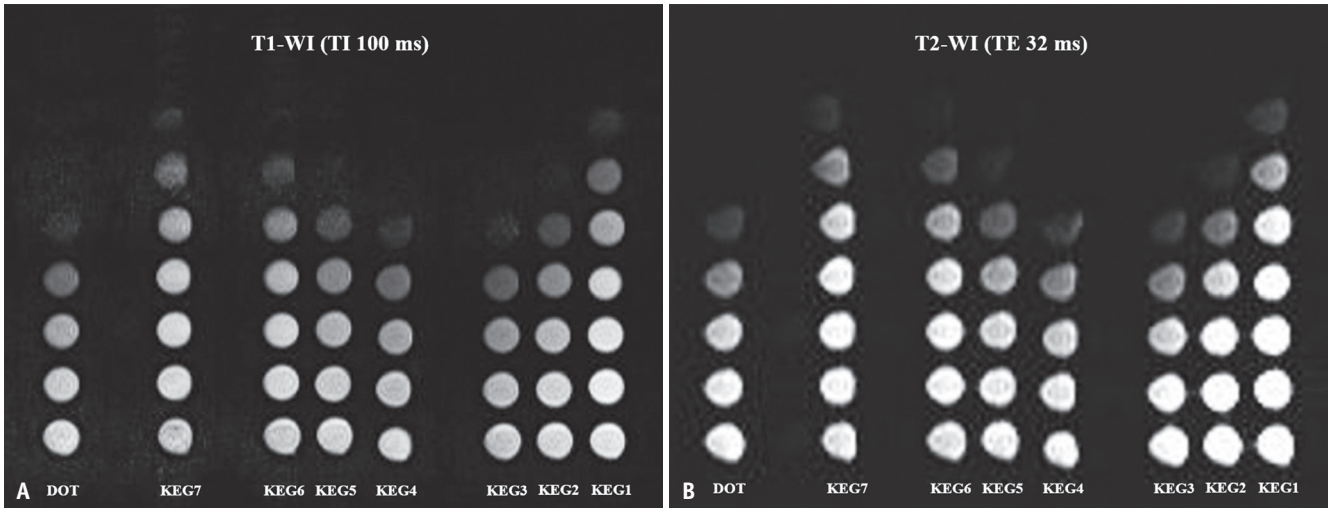

Fig. 1. Examples of T1-WI (A) and T2-WI (B) of the extremely small iron-based nanoparticles and Dotarem for T1 and T2 mapping.
The samples were prepared in descending order of concentration from top to bottom (undiluted solution, 1/2, 1/4, 1/8, 1/16, 1/32, 1/64, and 1/128). T1-WIs were acquired with an inversion-recovery turbo spin-echo pulse sequence, and the following parameters were used: TR = 4000 ms, TE = 14 ms, ETL = 2, slice thickness = 5 mm, inversion time = 25, 50, 75, 100, 150, 200, 250, 300, 350, 400, 500, 600, 800, 1000, 1500, 2000, 2500, 3000, and 3500 ms, matrix for phantom measurement = 228 x 384. T2-WIs were acquired with a multiple echo-spin echo pulse sequence, and the following parameters were used: TR = 5000 ms, TE = 16, 20, 32, 40, 48, 50, 60, 64, 80, 100, 150, and 200 ms, ETL = 1, slice thickness = 2 mm, matrix for phantom measurement = 160 x 256. ETL = echo train length, TE = echo time, TR = repetition time, WI = weighted image

https://doi.org/10.3348/kjr.2020.1455

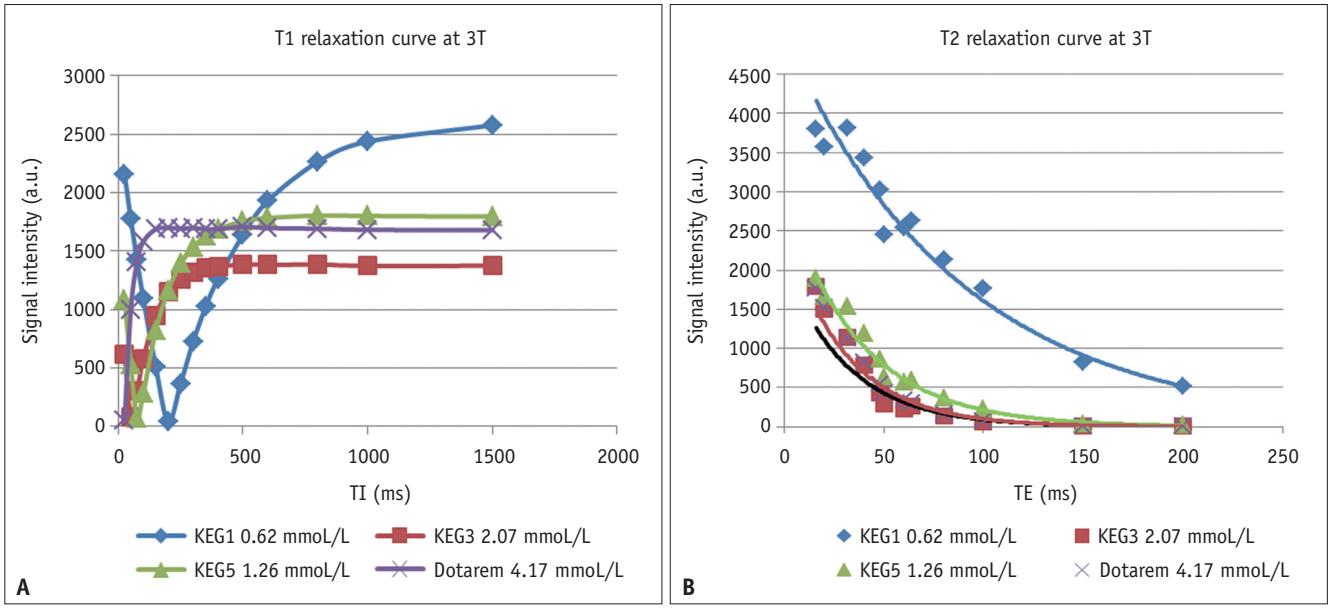

Fig. 2. Examples of T1 (A) and T2 (B) relaxation curves of the extremely small iron-based nanoparticles (KEG1, 3, and 5) and Dotarem obtained based on various T1- and T2-weighted images at 3T (dilution, 1/32). a.u. = arbitrary unit, TE = echo time, TI = inversion time

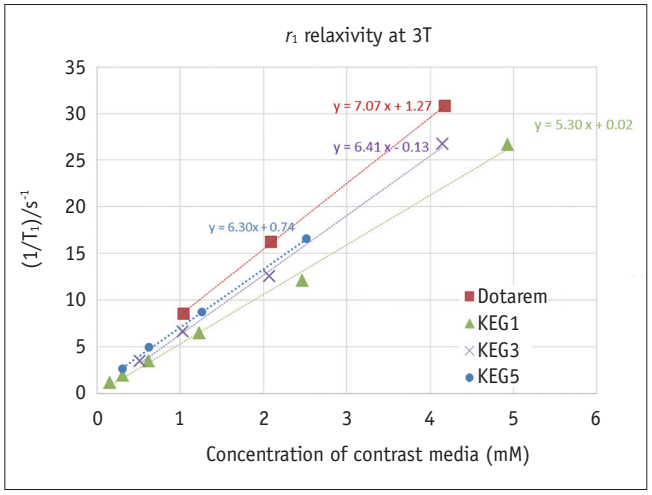

Fig. 3. Example of linear regression generated from a plot of the measured relaxation rate (1/T1) versus the concentration of the contrast media for the calculation of the r_1 relaxivity of KEG1, 3, and 5 and Dotarem at 3T.

In vivo Kinetics of the ESIONs

In the subjective image quality evaluation of the immediate post-contrast images, KEG5 showed an excellent contrast of the vascular lumen with well-visualized main aortic branches, allowing the entire course and luminal status to be fully evaluated with confidence. It also showed persistent vascular enhancement from the immediate post-contrast phase to the 90-minutes delayed phase. Dotarem® showed vascular enhancement only in the immediate post-contrast phase and was nearly washed out of the vascular structures after 5 minutes. KEG5 showed organ enhancement similar to that of Dotarem® in all regions on the immediate post-contrast images. On the 1-week follow-up images, KEG5 was nearly washed out of the vascular structures and organs (Fig. 4).

In vivo Cross-Over Experiment

All ESIONs and Dotarem® showed peak signal intensities on the immediate post-contrast images. The SI of Dotarem® showed an abrupt decrease, whereas that of all ESIONs showed a slight decrease on the 1-min post-contrast images. The SI of all ESIONs reached a plateau at post-contrast, and the vascular enhancement was maintained until 10 minutes post-contrast (Fig. 5).

All half-diluted contrast materials showed significantly lower signal intensities than did the non-diluted samples in all regions on the immediate post-contrast images ($p < 0.001$). On the 10-minutes post-contrast images, the half-diluted ESIONs showed a significantly lower SI than did the non-diluted samples ($p < 0.008$); however, there was no significant difference in the signal intensities between half-diluted Dotarem® and non-diluted Dotarem® ($p = 1.000$) (Tables 3, 4).

In terms of peak SI on the immediate post-contrast images, there was no significant difference between KEG3-S and DOT-S ($p = 1.000$); however, KEG3-S and DOT-S showed

https://doi.org/10.3348/kjr.2020.1455

Korean Journal of Radiology
KJR

Table 2. Relaxivities and Relaxivity Ratios of ESIONs and Gd-DOTA

	1.5T			3T			4.7T		
	r_1*	r_2*	r_2/r_1	r_1*	r_2*	r_2/r_1	r_1*	r_2*	r_2/r_1
KEG1	5.79	17.10	2.95	5.30	15.93	3.01	3.66	20.17	5.51
KEG2	2.95	17.72	6.00	2.38	13.61	5.72	1.41	18.03	12.79
KEG3	7.60	18.54	2.44	6.41	17.17	2.68	3.65	23.89	6.55
KEG4	4.86	12.19	2.51	3.52	11.98	3.40	2.29	16.67	7.28
KEG5	8.40	15.57	1.85	6.01	19.07	3.17	4.42	22.77	5.15
KEG6	6.73	29.43	4.37	5.77	21.68	3.76	3.64	29.99	8.24
KEG7	6.20	20.55	3.32	4.44	21.18	4.78	3.20	30.39	9.50
Gd-DOTA	7.74	8.64	1.12	7.07	8.71	1.23	2.75	3.46	1.26

*Values in $mM^{-1}s^{-1}$ and obtained at 22°C. ESIONs = extremely small-sized iron oxide nanoparticles, Gd-DOTA = gadoterate meglumine (Dotarem)

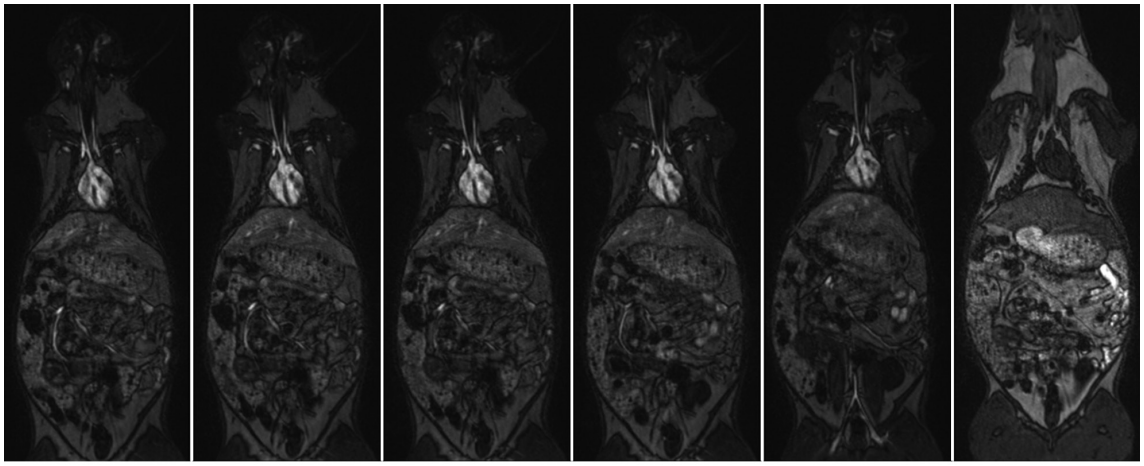

Fig. 4. *In vivo* post-contrast MR images of the ESIONs (KEG5) over time.
The ESIONs showed excellent contrast of the vascular lumen with the main aortic branches and persistent vascular enhancement from the immediate post-contrast phase to the 90-minutes delayed image. KEG5 was nearly washed out from the vascular structures and organs on the 1-week follow-up image. MR imaging was performed using the three-dimensional fast low-angle shot sequence, and the following parameters were used: repetition time = 2.8 ms, TE = 1.0 ms, flip angle = 20°, TE = 1.0 ms, slice thickness = 1 mm, number of excitations = 1, and field of view = 140 x 280. ESIONs = extremely small iron-based nanoparticles, MR = magnetic resonance, TE = echo time

significantly higher peak signal intensities than did KEG1-S in all regions ($p < 0.011$). On the 10-minutes post-contrast images, KEG3-S and KEG1-S showed significantly higher signal intensities than did DOT-S in all regions ($p < 0.001$) (Tables 3, 4).

DISCUSSION

MR contrast agents are generally categorized according to their effects on longitudinal (T1) and transverse (T2) relaxations, and their ability is referred to as relaxivity (r_1 and r_2). On MR images, fast T1 relaxation causes a bright SI, while fast T2 relaxation causes a dark SI. It has been reported that the parameter r_2/r_1 indicates whether the contrast agents become positive or negative. According to a previous study, bright T1-weighted images were observed at low r_2/r_1 values [15]. Therefore, the ideal T1 contrast agent needs a high longitudinal relaxivity (r_1) or a low r_2/r_1 value.

Common iron oxide nanoparticles are not appropriate for T1 MR contrast agents because the high r_2 of the iron nanoparticles derived from the innate high magnetic moment prevents them from being utilized as T1 contrast agents. However, in the nanoscale regime, the surface spin-canting effects of nanoparticles have a significant effect on their magnetic moment and MR contrast enhancement [16]. Small iron nanoparticles, such as USPIOs, show the T1 effect; however, the nanoparticles in previous reports were larger than 4 nm and still exhibited considerable magnetic moment. In contrast, the ESIONs in our study have 3–4-nm iron oxide cores and are expected to suppress the T2 effect

https://doi.org/10.3348/kjr.2020.1455

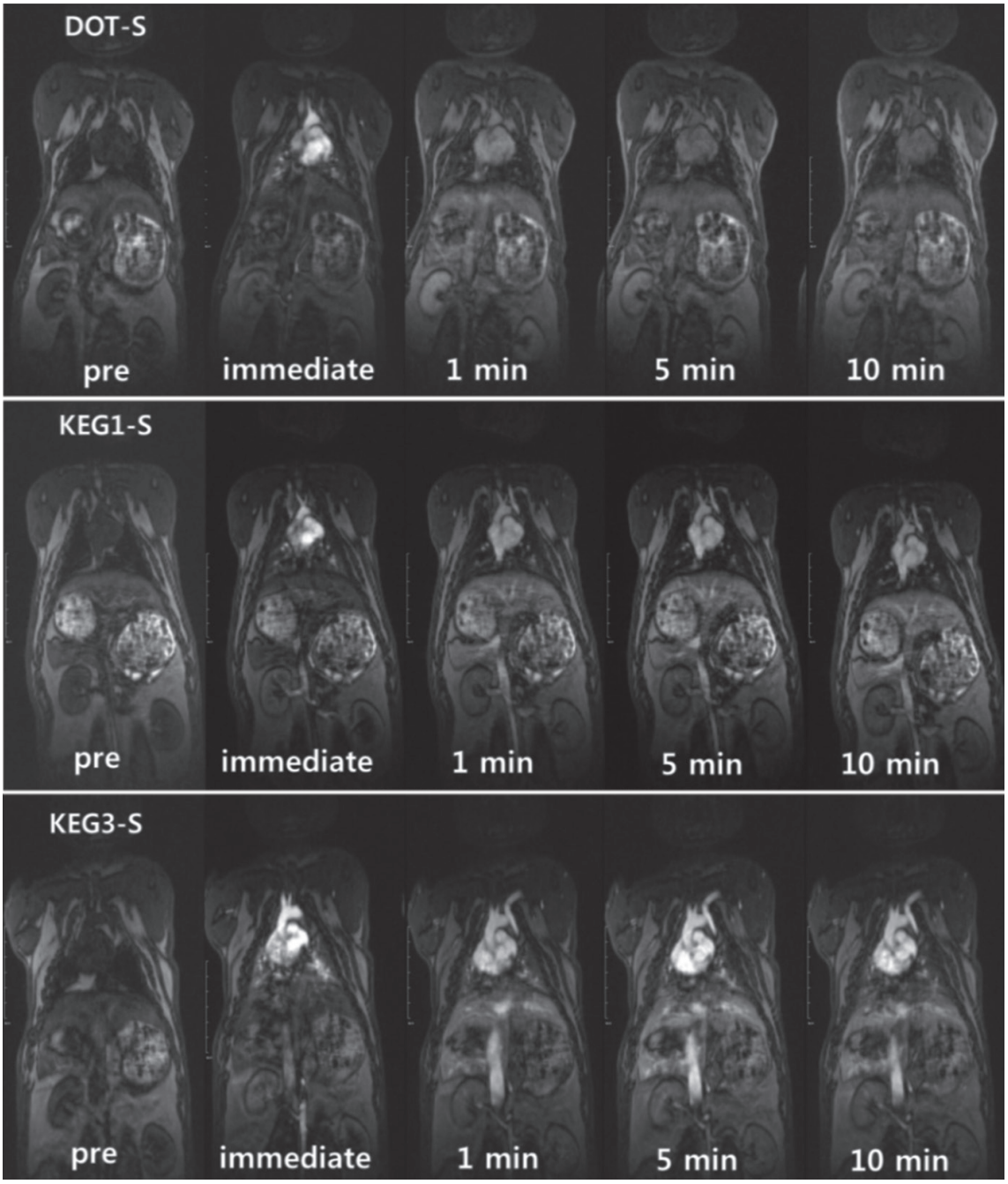

Fig. 5. *In vivo* cross-over experiment of the ESIONs and Dotarem. The ESIONs showed persistent vascular enhancement until 10 minutes post-contrast, whereas Dotarem showed an abruptly decreased enhancement on the 1-minutes post-contrast images. ESIONs = extremely small iron-based nanoparticles

with their small magnetic moment and have a strong T1 shortening effect owing to the nanoscale size.

Our experiment showed that the ESIONs had good physical characteristics as a T1 contrast agent, with a high r_1 value and low r_2/r_1 ratio. The ESIONs were synthesized via controlled thermal decomposition of the iron-oleate complex, and this synthetic technique led to uniformity in the size of the ESIONs, which is critical for the fine control of MR relaxivity [17].

In the phantom experiment, the relaxivity ratios (r_2/r_1) of the ESIONs increased with increasing magnetic field strength owing to the decreasing r_1 values. Theoretically, it may be expected that the T1 contrast effect of the ESIONs is lower at 4.7T than at 1.5T. According to previous studies on the effect of magnetic field strength on relaxivity, decreasing r_1 values with increasing magnetic field strength

https://doi.org/10.3348/kjr.2020.1455

Korean Journal of Radiology
KJR

Table 3. Between-Group Differences of the Signal Intensities on the Immediate Post-Contrast Images in Cross-Over Experiment

Region	*P*	Comparison	Estimate (Difference)	*P*	Adjusted *P**
Aortic arch	< 0.001	DOT-S vs. DOT-H	107.833	< 0.001	< 0.001
		KEG1-H vs. DOT-H	-56.000	0.001	0.010
		KEG1-S vs. DOT-H	14.167	0.380	1.000
		KEG3-H vs. DOT-H	-18.500	0.252	1.000
		KEG3-S vs. DOT-H	99.667	< 0.001	< 0.001
		KEG1-H vs. DOT-S	-163.833	< 0.001	< 0.001
		KEG1-S vs. DOT-S	-93.667	< 0.001	< 0.001
		KEG3-H vs. DOT-S	-126.333	< 0.001	< 0.001
		KEG3-S vs. DOT-S	-8.167	0.612	1.000
		KEG1-S vs. KEG1-H	70.167	< 0.001	< 0.001
		KEG3-H vs. KEG1-H	37.500	0.021	0.315
		KEG3-S vs. KEG1-H	155.667	< 0.001	< 0.001
		KEG3-H vs. KEG1-S	-32.667	0.044	0.659
		KEG3-S vs. KEG1-S	85.500	< 0.001	< 0.001
		KEG3-S vs. KEG3-H	118.167	< 0.001	< 0.001
Descending thoracic aorta	< 0.001	DOT-S vs. DOT-H	141.833	< 0.001	< 0.001
		KEG1-H vs. DOT-H	-67.667	0.001	0.019
		KEG1-S vs. DOT-H	67.000	0.001	0.021
		KEG3-H vs. DOT-H	6.833	0.740	1.000
		KEG3-S vs. DOT-H	138.167	< 0.001	< 0.001
		KEG1-H vs. DOT-S	-209.500	< 0.001	< 0.001
		KEG1-S vs. DOT-S	-74.833	< 0.001	0.006
		KEG3-H vs. DOT-S	-135.000	< 0.001	< 0.001
		KEG3-S vs. DOT-S	-3.667	0.859	1.000
		KEG1-S vs. KEG1-H	134.667	< 0.001	< 0.001
		KEG3-H vs. KEG1-H	74.500	< 0.001	0.006
		KEG3-S vs. KEG1-H	205.833	< 0.001	< 0.001
		KEG3-H vs. KEG1-S	-60.167	0.004	0.060
		KEG3-S vs. KEG1-S	71.167	0.001	0.011
		KEG3-S vs. KEG3-H	131.333	< 0.001	< 0.001

DOT-H, 0.05 mmoL/kg Gd-DOTA; DOT-S, 0.1 mmoL/kg Gd-DOTA; KEG1-H, 0.047 mmoL/kg KEG1; KEG1-S, 0.093 mmoL/kg KEG1; KEG3-H, 0.047 mmoL/kg KEG3; KEG3-S, 0.093 mmoL/kg KEG3. *Bonferroni's correction. Gd-DOTA = gadoterate meglumine (Dotarem)

are common in GBCAs [18]. Our results on the ESIONs and Dotarem® are consistent with previous findings. However, the MR signal depends on several MR-related factors and the concentration of the contrast material. Therefore, further studies should be performed in the clinical setting.

In the *in vivo* kinetic and cross-over experiments, the ESIONs showed compatible vascular enhancement compared to GBCAs on the first-pass MRA images and a similar organ enhancement pattern on the immediate post-contrast images in the objective and subjective evaluations. These results indicate that the clinical application of ESIONs as a blood pool contrast agent is reasonable and feasible. In addition, the ESIONs showed a persistent intravascular enhancement of more than 90 minutes, which made it possible to perform delayed imaging of vascular structures. ESIONs are hydrophobic, and the PEG ligand was introduced via a ligand exchange reaction to make the ESIONs dispersible in aqueous media [19]. Thus, the half-life of ESIONs in blood could also be increased by avoiding uptake by the reticuloendothelial system [20]. Thus, ESIONs can be used for repeated imaging and high-resolution imaging, which require long scan times. In a recent experimental study, ESIONs showed feasibility for potential use as a blood pool agent in coronary MRA with equivalent quality on first-pass images and better delayed images compared to GBCAs [21].

In terms of adverse effects, linear GBCAs can cause NSF in patients with renal dysfunction owing to toxic free gadolinium ions [22]. However, according to recent guidelines, the risk of NSF from the use of macrocyclic GBCAs is quite low, even in patients with acute or

 https://doi.org/10.3348/kjr.2020.1455

Table 4. Between-Group Differences of the Signal Intensities on the Post-Contrast 10 Minutes Images in Cross-Over Experiment

Region	*P*	Comparison	Estimate (Difference)	*P*	Adjusted *P**
Aortic arch	< 0.001	DOT-S vs. DOT-H	3.833	0.812	1.000
		KEG1-H vs. DOT-H	18.500	0.252	1.000
		KEG1-S vs. DOT-H	75.500	< 0.001	< 0.001
		KEG3-H vs. DOT-H	47.833	0.003	0.051
		KEG3-S vs. DOT-H	154.500	< 0.001	< 0.001
		KEG1-H vs. DOT-S	14.667	0.363	1.000
		KEG1-S vs. DOT-S	71.667	< 0.001	< 0.001
		KEG3-H vs. DOT-S	44.000	0.007	0.104
		KEG3-S vs. DOT-S	150.667	< 0.001	< 0.001
		KEG1-S vs. KEG1-H	57.000	0.001	0.008
		KEG3-H vs. KEG1-H	29.333	0.070	1.000
		KEG3-S vs. KEG1-H	136.000	< 0.001	< 0.001
		KEG3-H vs. KEG1-S	-27.667	0.087	1.000
		KEG3-S vs. KEG1-S	79.000	< 0.001	< 0.001
		KEG3-S vs. KEG3-H	106.667	< 0.001	< 0.001
Descending thoracic aorta	< 0.001	DOT-S vs. DOT-H	-0.833	0.968	1.000
		KEG1-H vs. DOT-H	27.500	0.184	1.000
		KEG1-S vs. DOT-H	126.500	< 0.001	< 0.001
		KEG3-H vs. DOT-H	68.833	0.001	0.016
		KEG3-S vs. DOT-H	201.833	< 0.001	< 0.001
		KEG1-H vs. DOT-S	28.333	0.171	1.000
		KEG1-S vs. DOT-S	127.333	< 0.001	< 0.001
		KEG3-H vs. DOT-S	69.667	0.001	0.014
		KEG3-S vs. DOT-S	202.667	< 0.001	< 0.001
		KEG1-S vs. KEG1-H	99.000	< 0.001	< 0.001
		KEG3-H vs. KEG1-H	41.333	0.046	0.697
		KEG3-S vs. KEG1-H	174.333	< 0.001	< 0.001
		KEG3-H vs. KEG1-S	-57.667	0.006	0.087
		KEG3-S vs. KEG1-S	75.333	< 0.001	0.005
		KEG3-S vs. KEG3-H	133.000	< 0.001	< 0.001

DOT-H, 0.05 mmoL/kg Gd-DOTA; DOT-S, 0.1 mmoL/kg Gd-DOTA; KEG1-H, 0.047 mmoL/kg KEG1; KEG1-S, 0.093 mmoL/kg KEG1; KEG3-H, 0.047 mmoL/kg KEG3; KEG3-S, 0.093 mmoL/kg KEG3. *Bonferroni's correction. Gd-DOTA = gadoterate meglumine (Dotarem)

chronic kidney disease; further, macrocyclic GBCAs can be administered when necessary, and there is no alternative test [23-28]. Nevertheless, the authors also recommend that informed consent should be obtained owing to the risk of developing NSF, and dialysis should be scheduled within 2–3 hours after GBCA administration in at-risk patients [29]. In addition, some researchers recently reported that the incidence of NSF decreased with regulatory actions and practice changes in the use of GBCAs [30]. From this point of view, there is a possible clinical application of ESIONs as an alternative contrast agent in patients with acute kidney injury or chronic kidney disease.

This study has some limitations. First, our experiments were performed with a limited number of animals. Although we adopted a cross-over experimental design to overcome the bias from the small number of samples, further experiments with large samples should be performed to support our results. Second, there were no prior *in vitro* toxicity tests of the ESIONs. Despite the advantages of ESIONs over GBCAs, safety concerns have been raised regarding the potential toxicity of iron oxide nanoparticles caused by oxidative stress owing to the excessive production of reactive oxygen species [31-33]. Although there were no acute adverse reactions in the animals during the experiment, further studies on the safety and long-term effects are required for clinical application in humans. Third, our experiments were performed using a clinical machine instead of an animal MR scanner. Therefore, there was a decrease in the spatial resolution, and the sites of MR signal measurement were limited to the large vessels.

https://doi.org/10.3348/kjr.2020.1455

Korean Journal of Radiology
KJR

In conclusion, the ESIONs with 3–4-nm iron oxide cores showed a good T1 shortening effect with relaxivity ratios (r_2/r_1) of 6 or less at 1.5T and 3T in the phantom experiments. Meanwhile, the ESIONs with 3-nm iron cores and 10-nm overall size (KEG3) showed comparable enhancement effect on first-pass imaging and superior enhancement effect on delayed imaging compared to the commercially available T1 MR contrast agent (Dotarem®) at 3T in the animal experiments.

Conflicts of Interest

The authors have no potential conflicts of interest to disclose.

Acknowledgments

This study was supported by a grant from the Hanwha Chemical Corp. The extremely small-sized iron-based nanoparticles were supplied from Hanwha Chemical Corp. The assistance of Bong-sik Jeon, PhD, Eung-gyu Kim, PhD, and Wan-Jae Myeong, PhD in some of the experiments is gratefully acknowledged.

Author Contributions

Conceptualization: Young Ho So, Whal Lee. Data curation: Young Ho So, Whal Lee, Pan Ki Kim. Formal analysis: Young Ho So, Whal Lee, Pan Ki Kim. Funding acquisition: Young Ho So, Whal Lee. Investigation: all authors. Methodology: Young Ho So, Whal Lee, Pan Ki Kim. Project administration: Whal Lee. Resources: Whal Lee. Software: Whal Lee. Supervision: Whal Lee. Validation: Whal Lee. Visualization: Young Ho So, Whal Lee. Writing—original draft: Young Ho So, Whal Lee. Writing—review & editing: all authors.

ORCID iDs

Young Ho So
https://orcid.org/0000-0002-1508-6869
Whal Lee
https://orcid.org/0000-0003-1285-5033
Eun-Ah Park
https://orcid.org/0000-0001-6203-1070
Pan Ki Kim
https://orcid.org/0000-0001-6006-0732

REFERENCES

1. Gozzi M, Amorico MG, Colopi S, Favali M, Gallo E, Torricelli P, et al. Peripheral arterial occlusive disease: role of MR angiography. *Radiol Med* 2006;111:225-237
2. Lim RP, Shapiro M, Wang EY, Law M, Babb JS, Rueff LE, et al. 3D time-resolved MR angiography (MRA) of the carotid arteries with time-resolved imaging with stochastic trajectories: comparison with 3D contrast-enhanced Bolus-Chase MRA and 3D time-of-flight MRA. *AJNR Am J Neuroradiol* 2008;29:1847-1854
3. Nael K, Fenchel M, Krishnam M, Finn JP, Laub G, Ruehm SG. 3.0 tesla high spatial resolution contrast-enhanced magnetic resonance angiography (CE-MRA) of the pulmonary circulation: initial experience with a 32-channel phased array coil using a high relaxivity contrast agent. *Invest Radiol* 2007;42:392-398
4. Prince MR. Gadolinium-enhanced MR aortography. *Radiology* 1994;191:155-164
5. Yucel EK. MR angiography for evaluation of abdominal aortic aneurysm: has the time come? *Radiology* 1994;192:321-323
6. Government of Canada. Gadolinium-containing contrast agents - Update on nephrogenic systemic fibrosis/nephrogenic fibrosing eermopathy (NSF/NFD) - Notice to hospitals. Healthycanadians.gc.ca Web site. http://healthycanadians.gc.ca/recall-alert-rappel-avis/hc-sc/2013/36711a-eng.php. Accessed August 15, 2018
7. U.S. Food and Drug Administration. FDA Drug Safety Communication: new warnings for using gadolinium-based contrast agents in patients with kidney dysfunction. Fda.gov Web site. https://www.fda.gov/Drugs/DrugSafety/ucm223966.htm. Accessed August 15, 2018
8. European Medicines Agency. Gadolinium-containing contrast agents. Ema.europa.eu Web site. http://www.ema.europa.eu/ema/index.jsp?curl=pages/medicines/human/referrals/Gadolinium-containing_contrast_agents/human_referral_000182.jsp. Accessed August 20, 2018
9. Khawaja AZ, Cassidy DB, Al Shakarchi J, McGrogan DG, Inston NG, Jones RG. Revisiting the risks of MRI with gadolinium based contrast agents-review of literature and guidelines. *Insights Imaging* 2015;6:553-558
10. Wang Y, Alkasab TK, Narin O, Nazarian RM, Kaewlai R, Kay J, et al. Incidence of nephrogenic systemic fibrosis after adoption of restrictive gadolinium-based contrast agent guidelines. *Radiology* 2011;260:105-111
11. Altun E, Martin DR, Wertman R, Lugo-Somolinos A, Fuller ER 3rd, Semelka RC. Nephrogenic systemic fibrosis: change in incidence following a switch in gadolinium agents and adoption of a gadolinium policy--report from two U.S. universities. *Radiology* 2009;253:689-696
12. Roch A, Muller RN. Theory of proton relaxation induced by superparamagnetic particles. *J Chem Phys* 1999;110:5403-5411
13. Antell H, Numminen J, Abo-Ramadan U, Niemelä MR, Hernesniemi JA, Kangasniemi M. Optimization of high-resolution USPIO magnetic resonance imaging at 4.7 T using novel phantom with minimal structural interference. *J Magn Reson Imaging* 2010;32:1184-1196
14. Ling D, Park W, Park YI, Lee N, Li F, Song C, et al. Multiple-

 https://doi.org/10.3348/kjr.2020.1455

interaction ligands inspired by mussel adhesive protein: synthesis of highly stable and biocompatible nanoparticles. *Angew Chem Int Ed Engl* 2011;50:11360-11365
15. Hifumi H, Yamaoka S, Tanimoto A, Citterio D, Suzuki K. Gadolinium-based hybrid nanoparticles as a positive MR contrast agent. *J Am Chem Soc* 2006;128:15090-15091
16. Jun YW, Lee JH, Cheon J. Chemical design of nanoparticle probes for high-performance magnetic resonance imaging. *Angew Chem Int Ed Engl* 2008;47:5122-5135
17. Kim BH, Lee N, Kim H, An K, Park YI, Choi Y, et al. Large-scale synthesis of uniform and extremely small-sized iron oxide nanoparticles for high-resolution T1 magnetic resonance imaging contrast agents. *J Am Chem Soc* 2011;133:12624-12631
18. Hagberg GE, Scheffler K. Effect of r_1 and r_2 relaxivity of gadolinium-based contrast agents on the T_1-weighted MR signal at increasing magnetic field strengths. *Contrast Media Mol Imaging* 2013;8:456-465
19. Na HB, Lee IS, Seo H, Park YI, Lee JH, Kim SW, et al. Versatile PEG-derivatized phosphine oxide ligands for water-dispersible metal oxide nanocrystals. *Chem Commun (Camb)* 2007;48:5167-5169
20. Pouliquen D, Le Jeune JJ, Perdrisot R, Ermias A, Jallet P. Iron oxide nanoparticles for use as an MRI contrast agent: pharmacokinetics and metabolism. *Magn Reson Imaging* 1991;9:275-283
21. Park EA, Lee W, So YH, Lee YS, Jeon BS, Choi KS, et al. Extremely small pseudoparamagnetic iron oxide nanoparticle as a novel blood pool T1 magnetic resonance contrast agent for 3 T whole-heart coronary angiography in canines: comparison with gadoterate meglumine. *Invest Radiol* 2017;52:128-133
22. Malikova H, Holesta M. Gadolinium contrast agents - are they really safe? *J Vasc Access* 2017;18:1-7
23. Schieda N, Blaichman JI, Costa AF, Glikstein R, Hurrell C, James M, et al. Gadolinium-based contrast agents in kidney disease: comprehensive review and clinical practice guideline issued by the Canadian association of radiologists. *Can Assoc Radiol J* 2018;69:136-150
24. Nandwana SB, Moreno CC, Osipow MT, Sekhar A, Cox KL. Gadobenate dimeglumine administration and nephrogenic systemic fibrosis: is there a real risk in patients with impaired renal function? *Radiology* 2015;276:741-747
25. Janus N, Launay-Vacher V, Karie S, Clement O, Ledneva E, Frances C, et al. Prevalence of nephrogenic systemic fibrosis in renal insufficiency patients: results of the FINEST study. *Eur J Radiol* 2010;73:357-359
26. Deray G, Rouviere O, Bacigalupo L, Maes B, Hannedouche T, Vrtovsnik F, et al. Safety of meglumine gadoterate (Gd-DOTA)-enhanced MRI compared to unenhanced MRI in patients with chronic kidney disease (RESCUE study). *Eur Radiol* 2013;23:1250-1259
27. Amet S, Launay-Vacher V, Clément O, Frances C, Tricotel A, Stengel B, et al. Incidence of nephrogenic systemic fibrosis in patients undergoing dialysis after contrast-enhanced magnetic resonance imaging with gadolinium-based contrast agents: the Prospective Fibrose Nephrogénique Systémique study. *Invest Radiol* 2014;49:109-115
28. Soyer P, Dohan A, Patkar D, Gottschalk A. Observational study on the safety profile of gadoterate meglumine in 35,499 patients: The SECURE study. *J Magn Reson Imaging* 2017;45:988-997
29. Schieda N, Maralani PJ, Hurrell C, Tsampalieros AK, Hiremath S. Updated clinical practice guideline on use of gadolinium-based contrast agents in kidney disease issued by the Canadian Association of Radiologists. *Can Assoc Radiol J* 2019;70:226-232
30. Attari H, Cao Y, Elmholdt TR, Zhao Y, Prince MR. A systematic review of 639 patients with biopsy-confirmed nephrogenic systemic fibrosis. *Radiology* 2019;292:376-386
31. Liu G, Gao J, Ai H, Chen X. Applications and potential toxicity of magnetic iron oxide nanoparticles. *Small* 2013;9:1533-1545
32. Storey P, Lim RP, Chandarana H, Rosenkrantz AB, Kim D, Stoffel DR, et al. MRI assessment of hepatic iron clearance rates after USPIO administration in healthy adults. *Invest Radiol* 2012;47:717-724
33. Sharifi S, Behzadi S, Laurent S, Forrest ML, Stroeve P, Mahmoudi M. Toxicity of nanomaterials. *Chem Soc Rev* 2012;41:2323-2343

https://doi.org/10.3348/kjr.2020.1455